Effects Of High Entropy Alloys Coating (HEAC) And Their Property Evaluation

Balaji. V and Anthony Xavior. M*

School of Mechanical Engineering, Vellore Institute of Technology, Vellore, Tamil Nadu, 632014, India

* *Corresponding author. E-mail: manthonyxavior@vit.ac.in*

Received: Oct. 03, 2023; Accepted: Jan. 04, 2024

High entropy alloy coating (HEACs) can be applied on metal, composite, and ceramics, including carbides and nitrides. HEACs are adopted in the automobile industries, particularly fuel injection systems, fuel filters, muffler surfaces, and aerospace sectors, including engine assemblies, landing gears, turbine blades, and rocket nozzles. As a matter of fact, the purpose of the coating is to minimize the wear rate, coefficient of friction, corrosion, diffusion, radiation rate, and increased resistance to impact. This review aims to study the performance of HEAs in comparison with the coating applied using conventional materials. Further, the influence of the fabrication methods and the parametric levels adopted on the implementation of the coatings will be presented. The performance of coating depends on the coating techniques, variations in the process parameters, and the coating thickness. Performance indicators (outcome) include the quantifiable parameters such as surface roughness, surface hardness, adhesive strength, surface energy, wear rate, and resistance to corrosion. A comprehensive review of the coating materials, techniques, and the process parameters will be presented in this review paper, along with the influence of all these aspects on the performance indicators. The suitability of HEAs coating on special applications will be addressed based on the HEAs unique properties.

Keywords: HEAs coating, Coating techniques, Coating performance, Corrosion

http://dx.doi.org/10.6180/jase.202411_27(11).0012

1. Introduction

A field of material science engineering currently being worked on is the creation of innovative alloying systems for energy-saving objectives. Based on the development of HEAs it is designed to develop various principle elements between 5 to 35 at% [1].

Based on HEAs rules followed by high entropy alloy coating (HEACs). These HEACs, which include carbides, oxides, nitrides, and borides, are applied to the surface of metals, composites, and ceramics. Surface modification techniques protect the substrate from external threats and enhance the substrate from the various working conditions. Depending on the working conditions (applications), the coating will either be thick or thin. To prevent the substrate from coating based on binding energy between the various elements followed by Gibbs free energy, $\Delta G = \Delta H - T\Delta S$. They were enhancing binding energy by increasing entropy. This entropy is one of the criteria for determining the types of phases, such as solid solutions or intermetallic compounds. Compared to intermetallic compounds, the solid solution phase must have a high mixing entropy [2].

Fig. 1 shown configurational entropy values of various alloy systems followed by periodic development. A single-phase solid solution is more helpful for improving the lifetime of metal coating. A single-phase coating improved the phase stability of the surface coating [3]. Wettability analysis is one of the surface characteristics that evaluate the bonding nature between the various elements on the surface. They aim to improve surface rigidity through me-

chanical interlocking, physical attributes through an atom or molecular interaction, chemical bonds through chemical reactions, and diffusion bonds [4]. The bonding behavior mainly depends on the energy density function in laser deposition methods. Increasing the energy density values due to higher power is predominant to better coat a substrate. Moreover, lower power ranges result in lower energy density and poor coating on the surface.

Made of HEACs: 1) Surface alloying, laser cladding, and remelting are laser deposition techniques. 2) Plasma cladding is a component of plasma deposition. 3) Thermal spray coating includes cold, plasma, and oxygen fuel spray. 4) Electrochemical deposition. 5) Vapour deposition techniques include PVD (Sputtering and Vacuum arc melting) and CVD. 6) Powder metallurgy includes hot and cold press sintering and mechanical alloying [5].

Coating performance based on Coating characterization. Like morphology Characterization using SEM and EDS. To predict the phase composition using XRD. Adhesive strength evaluation using a scratch tester. Surface energy evaluation using water contact angle goniometer. Surface hardness to measure the Vickers hardness tester. Friction and wear to evaluate pin-on-disc equipment. Evaluation of surface roughness using AFM. Laser-induced breakdown spectroscopy (LIBS) finds whatever elements are present in a material. Uncoated Al5083 substrate after $Al_{10.5}FeCu_{0.7}NiCoCr$ HEACs to achieve hardness of 750HV. It was around eight times greater than the uncoated substrate [6].

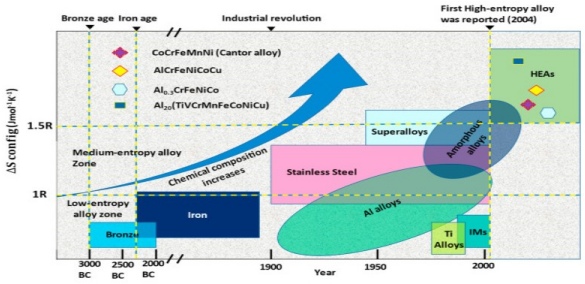

Fig. 1. Periodic development of HEAs [7]. Reuse with Journal Permission. Copyrights 2023, Elsevier.

2. Fabrication techniques of HEACs

2.1. Laser Deposition Techniques (LDT)

LDT enhances the surface of a specimen using a laser source. A laser is a source of heat that is applied to a substrate to create a cladding layer. Due to its extreme precision and tight tolerance limit, laser sources are used in modern times.

2.1.1. Laser Cladding (LC)

Surface processing is a hot spot of current research. The general way to deposit a coating on laser cladding is by heating and melting it as powder or wire through a substrate. As a result, LC offers a diverse range of coating options for a substrate, including new materials and repair work, i.e., tools, shafts, and turbine blades. Fig. 2 shown coating over the substrate with the help of a laser head and laser beam. Compared to other coating techniques, LC has very strong bonding, less heat absorption, and strong adhesion. The outcomes are controllability and reproducibility [8].

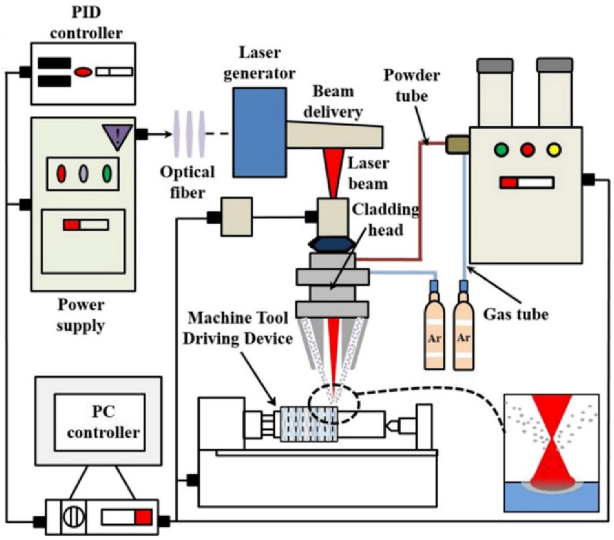

Fig. 2. The schematic diagram of laser cladding [9]. Reuse with Journal Permission. Copyrights 2023, Elsevier.

The initial temperature is applied to the substrate on processing routes to exchange energy. Followed by no additional phases are created. This stage is also called sensible heat. The next stage is the melting of the substrate to form a molten state. The final stage is substrate cooling and solidification. This solidification behavior depends on the cooling rate (r) versus temperature gradients (t). Microstructure was evaluated with the help of these results. The high $\frac{t}{r}$ promotes a planar structure, and the low $\frac{t}{r}$ promotes a dendritic structure [10]. Achieving a superior coating through LC requires consideration of several key parameters namely laser power, scanning speed, and beam size. In the metal coating process, coating aims to enhance the substrate life from the functional (wear) and natural hazards (environment). Compared to crystalline materials, the amorphous phases are better based on the wear

resistance applications. High amorphous phases have high hardness and wear resistance, but they affect a high-power source. Increasing binding energy is one of the primary key factors in improving coating performance. In that way, with the help of adding alloying elements like boron and carbides into reinforcement, $CoCrFeNi_xCu_{0.7}Si_{0.1}$ alloy system to prove that to increase the percentage of boron in that coating to increase the microhardness up to 502HV in the FCC phase. Reduce the amount of enthalpy needed to form a strong binding energy. Fe-B values are -37 kJ mol- 1 , B- Co is -34 kJ mol- 1 , B-Ni is -32 kJ mol-1, B-Cr is -45 kJ mol^{-1} and $B-Cu$ are $+1.76$ kJ mol^{-1}. Positive mixing enthalpy of copper between other elements results in more segregation [11]. Based on mechanical performance and lifetime of the coating surface, laser cladding is best compared to cast sample [12].

2.1.2. *Laser Remelting (LR)*

LR is part of surface treatment methods. Fig. 3 shows that LR will be preferred over improving the coating's microhardness compared to the non-remelted substrate.

Advantageous for wear resistance. As the name implies, remelting obtains homogeneity between the alloying system to improve the reheat of the billets six times [13]. This is proof that the sintered component has been reheated with the help of a laser source to obtain a more homogenous surface that results in improved hardness.

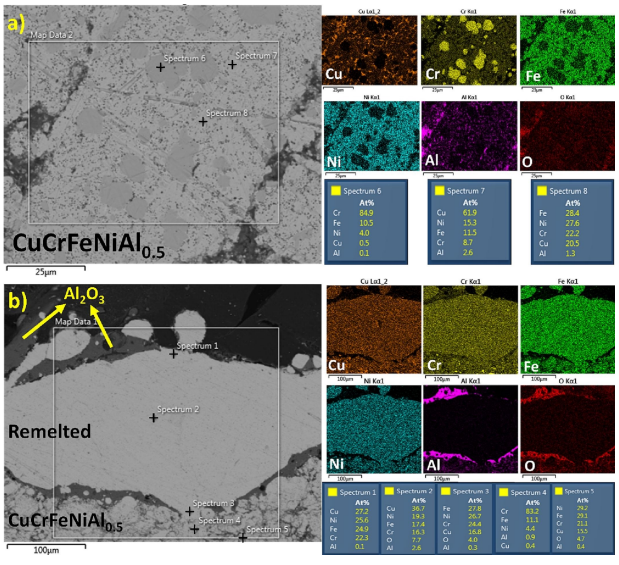

Fig. 3. Effects of LR on sintered component [14]. Reuse with Journal Permission. Copyrights 2023, Elsevier.

Based on the Marangoni effect, the heavy convective current passes the molten pool, producing rapid solidification and cooling. In XRD plots, narrow or major peaks denote a single-phase BCC or B_2 to form a dendritic region; moreover, intermetallic phases include an interdendritic region. Dendritic regions are less hard $(334 \pm 7HVN)$ than inter-dendritic regions $(409 \pm 9HVN)$ [13].

2.1.3. *Laser Surface Alloying (LSA)*

In LSA, the laser beam (heat source) is directly focused on the planning zone with Ar, Ni, He, etc. Nitrogen is highly resistant to wear and enhances its hardness compared to argon. Recently, laser surface alloying has become more attractive due to high efficiency, fast heating speed, and higher cost-saving reasons [15, 16]. Fig. 4 shows an improvement in the surface of the coating with the help of a laser beam via optical fiber. The effect of fast heating speed in Ti6A14V by fabrication of LSA coating to improve corrosion and high wear resistance [16].

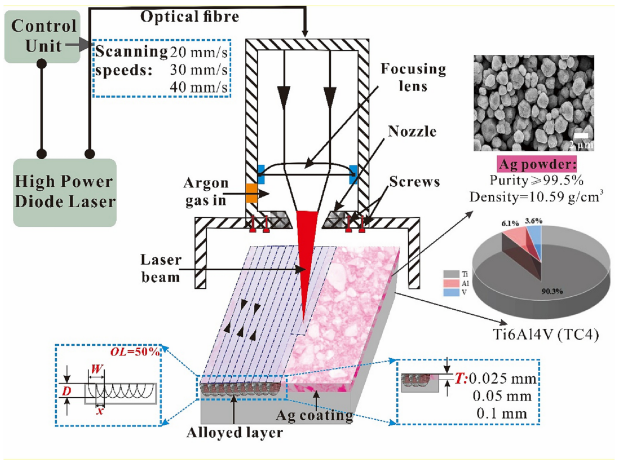

Fig. 4. The schematic diagram of laser surface alloying [17]. Reuse with Journal Permission. Copyrights 2023, Elsevier.

Nowadays, ceramic reinforcement is mainly used for alloying elements for metals such as Fe, Ti, Co, Cr, Al, and Cu. Ceramic reinforcement like TiC and Al_2O_3. The ceramic reinforcement is added to improve the modulus of elasticity and the uptrained low-density substrate and improve the Wt.% of TiC in the alloy system [18]. Coating of Fe-based CoCrCuAl HEAs system on Q235 substrate among them, Aluminium is higher atomic size difference $(0.143\ nm)$ for $Co(0.125\ nm)Cr(0.130\ nm)Cu(0.128\ nm)$ and $Fe(0.126\ nm)$ the effect of atomic size different higher to form a solid solution strengthening. In the above Febased CoCrCuAl system, copper has more positive enthalpy, so Cu has to create elemental segregation [18]. Rapid solid solution strengthening has to reduce grain growth, ultrahigh strengthening formation and grain boundary strengthening [19]. Intergranular phases in Co-based coating in HEAs enhance the grain boundary

strengthening result, which was prone to surface fracture [20]. Table 1 Shows more results of laser deposition techniques.

2.2. Electroless Coating Techniques

The coating process for electroless is a chemical process. Reduction of metal ions in a solution bath and deposition coating on the substrate. Through oxidation carried out in the same solution bath without the help of aquae-medium, there is no need for external current. Fig. 5 shows the experimental procedure for electroless coating process.

Electroless plating (silvering) bath solution based on various process parameters: 1) soluble salt of coating metals, 2) Reduction agents, 3) complexing agents, 4) Stabilizers, 5) Buffer agents, 6) Wetting agents, and 7) Controlled temperature. The bath preparation is based on acidic and alkaline (pH range 8 -10) ranges. But nowadays, from an industrial perspective, it is based on acidic baths because of the higher rate of chemical stability and the tendency for baths to decompose. Metal ions have the primary function of being the source of metals.

Reduction agents reduce the metal irons and get oxidized, i.e., 1) sodium hypophosphite- which has higher corrosion resistance as well as a low cost and common efficiency of 37% [29] . Amino boranes are used for Cu, Au, Co, nonmetals, and plastics. Sodium borohydride is mainly used for nickel plating and not for the aluminium substrate. Hydrazine is not applicable for high-temperature baths. Complexing agents must improve the coating quality (deposition rate) and preclude chemical bath decomposition, i.e., succinates and phosphates [30]. Exhaltants must enhance the plating rate, i.e., fluorides, succinates, and glycinates. Stabilizers have to minimize the decomposition rate and improve the life of the chemical bath, i.e., thiourea, cations, thulium, lead, and calcium. Buffer agents control the pH for the required period and improve the uniform plating rate of sodium acetate and sodium hydroxide rochelle salts. In this method, most metals, like nickel, copper, aluminium, silver, cobalt, palladium, gold, etc., are to be deposited. It focuses on electroless coating techniques and industrial usage based on developing unique properties. In this way, a coating based on nickel-phosphorus has to be achieved. In the acidic bath behavior of phosphorus, more attention is paid to enhanced wear and corrosive resistance.

The corrosion-prevention nature of multicomponent coating is superior to single-component coating [32]. The electroless process of nickel-based bath solution is followed by two methods: 1) Isothermal and non-isothermal. Non-isothermal approaches achieved a higher coating deposition rate at more than 180°C. This process deposition rate depends on the substrate and bath temperature. Higher substrate temperature increases deposition rate and coating hardness [33]. Corrosion for an upcoming research-based electroless coating based on a multicomponent alloy and its property improvement. The alternative of $Ni-P$ to $Ni-Fe$ coating to improve the wettability of some reinforcements like copper and graphite have very negative wettability [2].

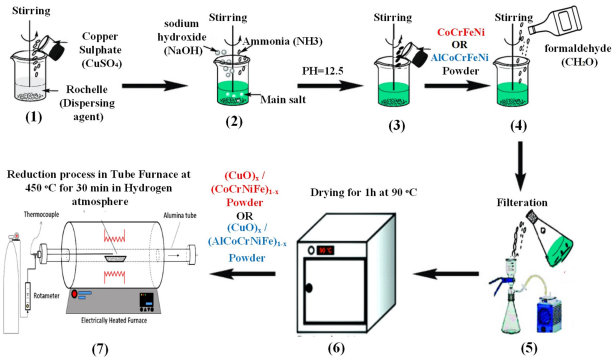

Fig. 5. Electroless coating process. Source from [31]. Reuse with Journal Permission. Copyrights 2023, Elsevier.

2.3. Plasma cladding

Plasma cladding methods are the most recent utilization methods for industrial applications. Because of minimizing manufacturing defects, low cost, suitable controllable machining parameters, and quality of coating [34]. Fig. 6 shows the working nature of the plasma cladding process. The quality of coating depends on raw material usage, but the limitation is its higher cost, and it is not suitable for industrial applications. It has to be replaced by using HEAs wires. Trible wire (TW) plasma cladding has recently been used because of its high efficiency at low coat. $TW-FeNiCr-Ti_x$ the percentage of x varies from $0, 0.5, 0.8$, and 1.0. The achieved hardness values are $137, 443, 769$, and $873HV$.

Higher Ti content achieved a higher hardness but an unstable friction coefficient [36]. The coating is based on the $AlCoCrFeNiCuSn_{x}$ over 35CrMo substrate. Increase the gradual percentage $(\text{tin}(x) = 0, 0.03, 0.05, 0.1$, and $0.2)$ of Sn in the HEACs system to increase the microhardness level and enhance the hardness and toughness result, representing better resistance to wear. But the opposite is like plasticity effects [37]. For that comparison of coating layers, microhardness is relatively higher than substrate. Because the outside layer of coating materials is to be performed to a higher degree of supercooling, that perspective enhances the fine-grain strengthening effects [38]. Table 2 shows more results of plasma cladding techniques.

Table 1. Some results of LDT

LDT	Alloying elements	Phases	Substrate	Microstructure	Coating thickness	Hardness (HVN)	Ref
LC	$Co_{34}Cr_{29}$ $B_{14}Fe_8Ni_8Si_7$	FCC + $FeAl_3$	45# Steel	Dendrite	-	-	[21]
LC	FeCoCrBNiSi	Amorphous + FCC	H13 steel	Equiaxed	0.2 mm	700 − 850	[22]
LC	AlCoCrFeNi/NbC	FCC+ BCC + NbC	Q235steel	Blocky + Equiaxed	1.2 mm	525	[23]
LC	$Al_{0.5}FeCu_{0.7}NiCoCr$	FCC + BCC	5083Al	Equiaxed+Columar	600μm	750	[24]
LC	6FeNiCoSiCrAlTi	BCC	Q235 steel	Equiaxed+Columar	1.2 mm	780	[25]
LSA	FeCoCrAlCu	BCC	Q235 steel	Dendrite	800μm	826	[26]
LSA	FeCoCrAlNi	BCC	304 S.S.	Equiaxed	0.6 mm	509	[27]
LSA	AlFeCrCoNi	BCC+ Al_3Ni+ $FeAl_3$	Al 1100	Columnar Dendrite	0.3 mm	-	[5]
LSA	FeCoCrAlCuNix	Dendrite	Pure Cu	FCC + BCC	500μm	522 − 636	[28]

Table 2. Some results of HEACs on various Plasma cladding methods.

	Alloying elements	Phases	Substrate	Microstructure	Coating thickness	Hardness (HVN)	Ref
Plasma cladding	FeCoNiAlCu	FCC + BCC	1045 steel	Equiaxed+ Columnar	1.0 mm	-	[39]
	CrCuFexNiTi	FCC+	Q235	Columnar	2.5 mm	650 − 730	[40]
	AlCoCrFeNiCuSnx	BCC + FCC	35CrMn	Dendrite	-	-	[37]
	FeCoCrNiNbx	FCC + BCC	Pure Ti	Dendrite	1.5 mm	500 − 600	[41]

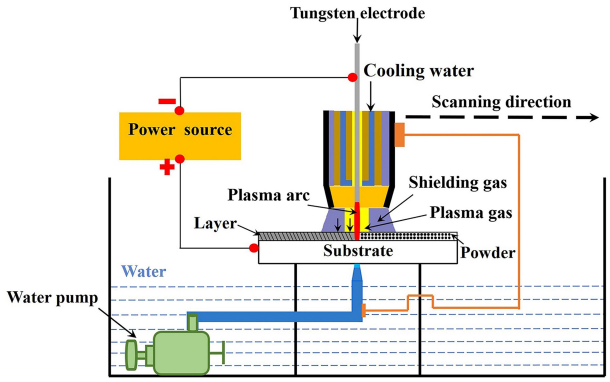

Fig. 6. The schematic diagram of the plasma cladding process [35]. Reuse with Journal Permission. Copyrights 2023, Elsevier.

2.4. Thermal spray coating

Thermal spray or thermal barrier coating is a novel method for preparing HEACs. The coatings are primarily used in high-temperature applications, such as gas turbine blades and engine exhaust zones. It includes two ways: 1) Plasma spray, 2) Oxy-fuel spray, and 3) Cold spray coating.

2.4.1. Plasma spray coating (PS)

Plasma spray techniques are one of the thermal spray coating methods. The coating was applied to a substrate using powder at the desired plasma jet velocity. The coating is applied to metal, ceramics, and cermet. These coatings are intended to offer functional qualities like thermal insulation and biocompatibility. It also supported enhanced wear and corrosion protection. Application perspectives: bioceramics coatings of zirconia-titania-silica used in implant applications coating over liquid metal battery surfaces and to prevent fretting wear, seal ring grooves in the compressor area of aero-engine turbines with tungsten carbide or cobalt. The coating efficiency depends on parameters like arc current, arc voltage, gas flow rate, standoff distance, vacuum atmosphere, and powder feed rate. Stand-off distance is related to the efficiency of the coating. To increase the plasma spray coating efficiency, decrease the standoff distance. The effect of coating performance under oxygen enhanced the mechanical characteristics. The oxygen-supplied conditions have to vary from 1) stationary or inert and 2) spread at the time of coating, resulting in the bumping of oxygen into metal powder. $Ni_{50} - Ti_{50}$ at% coating is based on NiCoCrAl bond coat powder following these conditions. Evaluation of Oxygen spread type coating higher oxygen

affinity for Ti [42]. Ti plays a significant role in the biomedical field in replacing hip and bone orthopedic applications. Bioceramics coating was preferred over Ti substrate with the help of plasma spray methods [43]. An inspection point of view in plasma spray coating in X-ray micro CT scans is used nowadays. Followed by liquid metal barrier coating, which mainly eliminates the corrosion rate to evaluate using a CT scan.

2.4.2. *High-velocity Oxy-fuel spray coating (HVOF)*

An oxygen and fuel mixture is injected into a combustion chamber and ignited using a thermal spray method called high-velocity oxygen fuel (HVOF) coating. The combustion chamber's output gas is ejected out a nozzle at supersonic speeds while being produced at an extraordinarily low temperature, high pressure, and velocity $(> 1000\ \mathrm{m/s})$ [44]. Spraying fuels are mainly used for hydrogen, acetylene, kerosene, natural gas, methane, etc. Strong wear resistance, thick or thin coating, and high gas velocity to improve a higher bonding, low permeability in nature, and microhardness are the causes of metal powder sprinkled over a substrate at a high temperature. HVOF quality depends on the following:

1. The particles added to the gas stream must be accelerated to impact the target at high speed.

2. Heat must be transmitted for the particles from the gas stream to melt before colliding [44].

2.4.3. *Cold spray coating (CS)*

Cold spray coating is additionally known as a cold-gas dynamic spray. The basic work of the CS coating is that the high velocity of the powder is adhered to the substrate under perfect plastically deformed conditions at high-pressure gas jets to move faster, bonding the coating at supersonic speed. Applying coatings to the surface of bulk material is primarily expected to enhance the flexibility of coating on the substrate, increase its affordability, and provide an efficient way to improve the material's properties, primarily to increase its usefulness and prolong its useful life. Based on this, cold spray coating should be satisfied under low temperatures and below the melting point of the base powder so no phase transformation occurs in bulk materials. Kinetic energy and supersonic velocity attract powder particles to the substrate at lower temperatures.

Thermal spraying methods also reduce the residual stress acting on a surface [45]. The coating quality mainly depends on eliminating defects from the surface, so porosity is one of the major contributions to creating defects in the coated surface. Recent days in failure analysis of HEACs based on elimination porous in the coating are focused, which means low porous to enhance the mechanical properties. CS coating over the substrate in the form of pure elements and composite form. Composite coating forms minimize the porous level, enhancing surface adhesion strength compared to pure element coating. Moreover, CS methods form some microvoids over the coated surface [46]. Coating over soft aluminium AA6060 and hard 1.0037 steel substrate in Ti_2AlC coating to consider microhardness and standard deviations in this literature work. The microhardness values of the substrate AA6060 were $90.9 \pm 5.1HV_{005}$ and 1.0037 steel $197.5 \pm 7.4HV_{0.05}$. After coating, microhardness increases from 608.4 to $118.5HV_{0.05}$ and 786.7 to $130.7HV_{0.05}$. The result delivered based on coating substrate hardness is an important criterion for the final result [45].

From that perspective, it eliminates oxidation and reduces the residual stress at lower temperatures. Cold spray coating of AlNiCoFeCr equiatomic ratio reinforced with TiB_2 between the various temperature limits of 200,300 , and 450°C among these levels to achieve microhardness of $5.3 \pm 0.3, 6.1 \pm 0.2, 6.9 \pm 0.2$GPa and to achieve a fracture toughness of 300°C specimen 2.6 ± 0.3 and 450°C in $3.8 \pm 0.1 MPam^{0.5}$ solid state coating at 450°C has higher possible result achieved [45]. The common limitations obtained in CS coating are lowtemperature functioning and plastic deformation, which are essential for CS. So, CS is not suitable for ceramics-based coating. It revealed ceramic-based CS coating over the substrate compared to pure Al blended $Al + TiC$ and satellite $Al + TiC$. Pure Al was less porous than the satellited powder process (mixing 88wt% of Al and 12wt% of TiC), meaning pure Al has high plasticity and does not rebound over the substrate. Furthermore, $Al + TiC$ was added to a ceramic with less plasticity to achieve more particle rebound and a highly porous surface [4]. The particles rebound, and one of the reasons is an improper flattening ratio (FR). However, the FR has been associated with predicting the performance of wear and fracture toughness. A comparative study of the Ti-6Al-4V matrix over varying wt% like $6Al - 10Al - 50Al$ must be used because Al has an FCC crystal structure with low yield and higher plasticity. FR has Ti-6Al-4V-6 wt.% Al attained 1.76, Ti-6Al-4V- 10Wt% Al attained 1.97 , and Ti-6Al-4V- 50 wt. %Al attained 1.94. The result showed that this alloy system with increasing FR had poor wear resistance and good fracture toughness [46].

Conclude over three types of thermal spray coating. HVOF coating is less porous to the coating surface and has higher microhardness, wear resistance, and higher density. Majorly, higher-density materials have higher mechanical

properties like hardness and toughness. CS is the best choice for FCC-based materials. Plasma spray coating has a high deposition rate to achieve more wear resistance. Table 3 shows more results of plasma cladding techniques.

2.5. Powder metallurgy (PM)

HEACs made of powder metallurgy are the easiest and least cost-consuming methods, and there is no need for temperature, which results in minimizing the phase separation behavior. There are two methods: 1) Mechanical alloying (MA) and 2) Hot press sintering. MA is a solid-dry milling and semi-solid state-wet milling process in equilibrium and nonequilibrium composition. The critical consideration of MA is to add more than two elements in different particle sizes after MA to get fine and homogenous mixtures. MA's effects change the particle from micro to nano size. The nano-size particles are visible to address the mechanical properties improvement like wear resistance, reduce the friction coefficient, and also reduce the corrosion rate to improve the electromagnetic properties. Also, other perspectives about MA enhance bonding during metal compaction.

Based on the material's crystal structure, for the higher time of MA, the crystal structure has to change from BCC to FCC and FCC to BCC or form intermetallic compounds based on alloying additions. To study the Al and Mn behavior of HEACs of FeCoNiCrAl and FeCoNiCrMn after atmospheric plasma spray coating to evaluate microhardness from particle changes from micro to nano size transformation to enhance the hardness from Al based HEAs to be achieved from 550.1 HV_{100gf} and Mn-based HEAs 440.9HV_{100gf}. The binding nature of Al and Mn with oxygen is low and easy to form in oxide [53]. The study focused on electromagnetic wave absorption behavior after MA on FeCoNiCrAl HEACs for 10 to 70 hrs. Frequency ranges from 2 to 18 GHz and is based on reflection loss to decide whether HEAs are suitable for these applications or not. The test is carried out in a vibrating sample magnetometer. The stability of MA is to be achieved on 60 to 70 hours of milling, which means that after 70 hours, no changes happened in the metal powder. The resulting point of view is to achieve minimum reflection loss (RL) to attain maximum microwave absorption capacity. Based on this statement, the preparation of FeCoNiCrAl alloying elements will perform an RL of -35.3 dB at 10.35GHz.

These results are compared to TiC/Tip RL of -18.9 dB and graphene/ $BaFe_{12}O_{19}/CoFe_2O_4$ of RL of -32.4 dB. All the results address the HEAs coating/powders to absorb the microwaves [54]. During MA, the effect of oxidation is essential for property evaluation. Ti-4Al-6V substrate over $Cr-AlSi_{12}$ coating fabrication routs on MA at different weight ratios like 70:30, 65:35, 60:40, and 55:45. Purpose of selection of $AlSi_{12}$ is quickly homogenized with the help of MA. Results have to improve the restriction of microhole formation on the top surface, and $AlSi_{12}$ is also called silumins. Cr is located over the inner layers and eliminates its formability because it is brittle.

The purpose of the surface coating is to minimize the oxidation rate on the substrate. Ti quickly affects the oxidation over 600°C [55]. For the above study, 60wt%$Cr-40$wt% of $AlSi_{12}$ achieved a lower oxidation rate [56]. Routs of PM on another method are vacuum hot press sintering (VHPS), which has a controllable temperature utilized to make a sintering process. Under vacuum conditions, the sintering process is carried out to reduce the oxidation level. Effects of copper addition on CoCrFeNi and $CoCrFeNi-Cu$ HEACs over on Q235 substrate. Adding copper to the high entropy alloying system minimizes the redox reaction at lower vacuum conditions. Also, comparative results have been visible to address the effect of Cu with HEAs to improve the bonding behavior to the Q-234 substrate, but the limitation part is compared to without the addition of Cu have to achieve higher microhardness because Cu has FCC crystal structure [57]. Based on PM, which will be developed daily in this PM-HEA, this is one of the broad opportunities for additively manufactured HEAs components, followed by characteristic thermodynamic modeling and analysis techniques. Another feature is the oxidedispersed strengthening of HEAs components. Table 4 shows more results of powder Metallurgy techniques.

3. Mechanical characterization of HEACs

3.1. Friction and Wear Behaviour of HEACs

Modern material processing techniques enhance wear and minimize friction between the matching parts. From that perspective, HEACs perform better than conventional coatings to improve the wear resistance rate in automotive and industrial applications. 1) Hard coating, i.e., the substrate has TiN coating over different substrates on TiAlN, TiNbN, and TiCN; among them, TiCN coating has a lower friction coefficient and high wear resistance because C and N enhances the solid solution in interstitial form. These types of hard coating are primarily applicable for high-temperature applications like cutting tools, engines, and cogwheels [62]. 2) Solid lubricant coating - used for low-friction applications.

The wear behavior is evaluated with the help of SEM, Raman spectroscopy, and EDS. In recent metal matrix composite processing techniques, reinforcement (RF) was added to the matrix to enhance the wear property behavior,

Table 3. HEACs on various Plasma cladding methods.

Spray techniques	Alloying elements	Phases	Substrate	Micro Structure	Coating thickness (μm)	HVN	Ref.
PS	AlCoCrFeNi	FCC + BCC+ $Al_2(Cr,Fe)O_4$	Mild steel	Lamellar	-	413	[47]
PS	MnCoCrFeNi	FCC + BCC+ Fe_3O_4	Mild steel	Lamellar	-	442	[47]
PS	AlCoCrCuFeNi	BCC + FCC	Pure Mg	Lamellar	275	-	[48]
PS	AlCoCrFeNiTi/Ni 60	FCC + BCC	316SS	Lamellar	-	195	[48]
HVOF	$Ni_{0.2}Co_{0.6}Fe_{0.2}CrSi_{0.2}AlTi_{0.2}$	BCC + Cr_3Si	Incoloy 800H	Pancake layer	1500	400 – 800	[49]
HVOF	$Al_{0.6}TiCrFeCoNi$	BCC	ATSM A572	Lamellar	300	850	[40]
HVOF	AlCoCrFeNiTi	BCC	S235 steel	Lamellar	210	810	[50]
CS	FeCoNiCrMn	FCC	6082Al	-	1500	368	[51]
CS	FeCoNiCrMn	FCC	304SS	-	1500	258 – 302	[52]

Table 4. HEACs on Powder Metallurgy

PM	Alloying elements	Phases	Substrate	Coating thickness (μm)	Surface Hardness (HVN)	Friction Coefficient	Ref
VHPS	CuZrAlTiNi	FCC + BCC + $AlNi_2Zr$ or Amorphous	T10 steel	900	943	0.70	[58]
VHPS	CoCrFeNi	FCC	Q235 steel	700	450	0.38	[59]
VHPS	CoCrFeNiCu	FCC	Q235 steel	700	400	0.60	[59]
MA	AlCuNiFeCr	FCC	stainless steels	10 – 40	803	-	[60]
MA	Cr_x% of $AlSi_{12}$	-	Ti-6Al-4V	150	305 – 465	-	[57]
MA	CrMnFeCoNi	FCC	Q235 steel	180	-	-	[61]

followed by RF in metal, carbides, boride, nitride silicide, etc. Comparative study of with and without the addition of 0.5wt% of sulfur (S) to CoCrFeNi alloying system with S achieved an average friction efficiency of 0.41 and wear rate of 5×10^{-5} mm^3Nm^{-1} and without S, the average friction coefficient 0.6 and wear 24 $\times 10^{-5}$ mm^3Nm^{-1} at 800°C. The result shows good wear resistance and hard materials have a lower friction coefficient [63].

The RF has a significant role in improving mechanical properties. In that way, the same crystal structure between the matrix and RF has strong metal bonding at the interface because of the reduced wear rate. Meanwhile, ceramic RF in MMCs has high strength and wear resistance but lower toughness [64]. Effects of aluminium on the copper RF in various wt% from 0, 6, 15, and 27 from solid solution (SS) and T3 heat conditions. Increased wt% copper also rose agglomeration and enhanced the uniform powder particle distribution in both SS and T3 conditions. SS and T3 conditions improve the wt. % of Cu in SS rods and have a higher wear rate than T3 conditions [65]. Adding elements' effects to the HEAs fine-grained structure has high wear resistance compared to a coarse structure [65].

The impact of tungsten (W) addition for $CoCrFeNiW_X$ on AISI 1045 substrate on the production of HEAs coatings in the laser cladding method examination of wear behavior on the percentage of $W(0, 0.25, 0.50, 1.0)$ addition and temperature differences (room temperature, $200, 400, 600, 800$°C). CoCrFeNiWX addition increases hardness up to 374.4 HV and CoCrFeNi 182.7HV through the coating effect. 200°C is the optimum temperature for minimizing the wear achieved for 2.7×10^{-5} $mm^3/N \cdot m$. With the help of this optimum temperature, it minimizes the microcrack formation and reduces the wear debris [66]. Singlephase HEAs coating is inferior to dual-phase HEAs coating in high-temperature applications. Furthermore, dual-phase coating performs worse at room temperature than single-phase HEAs coating [67]. Additionally, the wear mechanism uses the Pilling Bedworth Ratio (PBR) to

identify the oxides present across the coating's volume variation. Better coating wear resistance under $1 < \text{PBR} < 2$ conditions. Mo, Nb < 2PBR[68].

3.2. Effect of Toughness on HEACs Surface

All the working conditions of the alloy system have to improve the lifetime of a substrate, followed by the externally hard and internally toughness nature. Fig. 7 Illustrate effects of elastic strain limit to fracture toughness. Based on the strengthening mechanism followed by HEACs. The major considerable factors for the improvement of strength and toughness were stress intensity factor K, $\frac{H}{E}$ elastic strain limit, resistance to plastic deformation (H− hardness, and E- elastics modulus), and plasticity index (Φ) [67]

$$\Phi = \frac{E}{H}\left(\frac{\sigma}{\beta}\right)^{\frac{1}{2}} \tag{1}$$

σ = surface roughness and β = asperity radius.

The high plasticity index is a small contact stress indices. The Φ is inversely proportional to the $\frac{H}{E}$ values. The material behaves with no plastic deformation. It has to obey high toughness in nature. Another one is the Coating hardness analysis method, which is correlated with sphere-on-flat hertzian contact analysis (P_{max}) [67]

$$\text{Pmax} = \frac{1}{\pi} \times \left(\frac{6NE^2}{R^2}\right)^{\frac{1}{2}} = 0.578\left(\frac{NE^2}{R^2}\right)^{\frac{1}{3}} \tag{2}$$

Pmax $< \sigma_y$ in this condition, no plastic deformation occurred. Higher $\frac{H^3}{E^2}$ value, less plasticity, and more toughness [67]. The uncoated substrate's fracture toughness values were determined by observing specific deflection during the bending test, which allowed for the development of surface fractures to be evaluated qualitatively. Also, fracture toughness values vary between different layers of coating, i.e., single and multilayer coating.

Temperature is one of the influencing factors for functioning fracture toughness in metal coating. They are using some techniques to find the fracture toughness. 1) Nanoindentation- highly preferable for BCC phases, 2) scratch test, 3) micro cantilever bending method, 4) focused ion beam methods, etc. This was followed by an evaluation of fracture toughness in the addition of 4.5 at.% of silica in the single-layer hard coating on CrAlN and CrAlSiN in high-temperature applications (metal cutting operations) using magnetron sputtering methods. Coating thickness from 3.6μm of CrAlN and 4.5μm of CrAlSiN Influence of Si into the alloying system to form a new crystal growth in columnar form and enhance mechanical properties and crystal structure in nanocrystalline form. Also, low dislocation density was achieved [68].

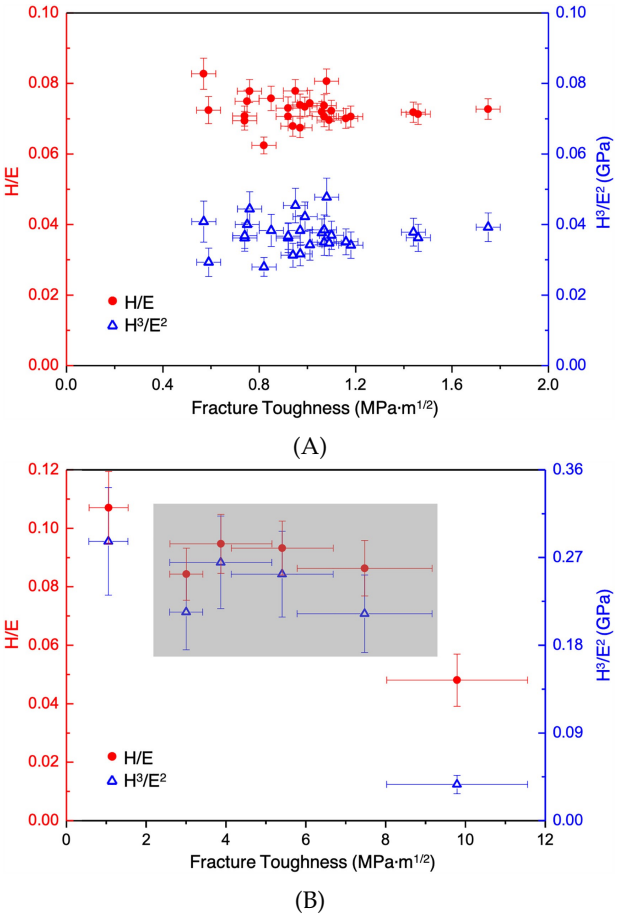

Fig. 7. Effects of fracture toughness on A) aluminosilicate and B) VC, W [67]. Reuse with Journal Permission. Copyrights 2023, Elsevier.

For multilayer composite coating of metal and ceramics to attain a high toughness and considerable amount of hardness in Fe/VC coating in 550 nm thickness in various thickness fractions 0.6 to 0.9 . Evaluate the fracture toughness $Fe_{0.6}/VC_{0.4}$ attained 1.7MPam^{-5} and $Fe_{0.9}/VC_{0.1}$ attained 3.2 MPam^{-5} increase the Fe thickness to improve the toughness [69]. Effect of various boride layers ($(CoFe)_2$ B, $(Fe_{0.4}Mn_{0.6})$ B, $(Cr_{0.4}Mn_{0.6})$ B, (Cr_2Ni_3) B) in $Co_{1.21}Cr_{1.82}Fe_{1.44}Mn_{1.32}Ni_{1.12}$ $A_{10.08}$ $B_{0.01}$ HEAs substrate. For fracture toughness evaluation under nanoindentation crack-based methods K_c [70],

$$K_c = \sqrt{G_c E} \tag{3}$$

The boride coatings were subtracted under different temperature conditions to increase the temperature to 900°C, 950°C, and 1000°C. Increased temperature values

also increase the boride thickness. Increasing the boride thickness also increases the hardness of the coated substrate [70].

3.3. Effect of Corrosion Resistance in HEACs

The performance of a surface coating is to prevent environmental hazards (aqua, acid, temperature, pressure) to the substrate. It also enhances the tribological and anti-corrosion properties. The effect of corrosion changes in the phase structure, segregation among the elements, reduction of the passive film nature, and dissolution kinetics [71].

In HEACs, elements such as Co, Cr, Ni, Ti, Al, Cu, and Mn have non-negative corrosive collaboration among the multiple components in different alloying elements. Various methods are used to test and evaluate the coated surface, like the potentiodynamic polarization test, to obtain parameters 1) corrosion current density $(i_{\text{coff}}, 2)$ corrosion potential $(E_{\text{coff}}), 3)$ pitting potential (E_{pit}) or breakdown potential $(\text{E}_{\text{b}}), 4)$ passive current density (i_{pass}) was done on 3.5 wt.% of NaCl solution [72]. Cu and Mo to reduce the pitting corrosion. The coating of $FeCoCrCuAlSi_{0.5}$ has a similar microstructure, and no pitting corrosion was absorbed in the effect of the addition of Cu [38]. Coating made on electroless methods, In the comparative study of the addition of Cu to CoCrFeNi and AlCoCrFeNi in this alloying system, corrosion rate (CR) of $Cu - CoCrFeNi$ attained 0.297 to 1.84 mm^{-1} year $^{-1}$ and $Cu - AlCoCrFeNi$ attained 0.03 to 0.093 mm^{-1} year $^{-1}$ in addition of Cu to the Al, reduce the CR. Because of the highly passive region (which impedes the progression of corrosion), the form of Cr is transferred into Cr_2O_3 to reduce the CR, Cu nanoparticles are distributed uniformly, and the BCC phase has better CR than FCC in electroless coating conditions [31]. Different fabrication routes of $CrCuFeNiA_{10.5}$ made of sintering techniques and $CrCuFeNi_{10.5}Si_{0.5}$ made of laser remelting

(LR), and to evaluate corrosion rates and their types. In sintered components, corrosion occurs along the edges of the grains, so for this reason, the sintering substrate forms intergranular corrosion. LR of $CrCuFeNiAl_{0.5}Si_{0.5}$ The grain boundaries should be removed or invisible to the grains because of the more homogenous distribution of particles with the help of a laser source. Therefore, the LR substrate forms a pitting-type corrosion, and oxide layers are on the surface. Compared to the sintering method, LR has a lower corrosion rate. The effect of single crystal structure BCC, FCC, and amorphous structure is a more uniform microstructure and decreases the pace of corrosion [73].

4. Future scope:

In HEACs, the behavior of fatigue failure analysis and residual stress analysis are not yet addressed significantly which can be focussed in future.

5. Conclusion

Despite the abundant work in conventional coating and its improvement, HEACs have had an essential place in the 21^{st} century. There has been significant progress, and it continues to generate substantial new scientific concepts and new research challenges identified by this work; various types of coating and its effects and various reinforcements used in coated surfaces, mechanical characterization, and favourable and unfavourable cases are discussed in this manner.

References

[1] M.-h. Tsai, J.-w. Yeh, M.-h. Tsai, and J.-w. Yeh, (2014) *"High-Entropy Alloys :A Critical Review High-Entropy Alloys : A Critical Review"* **Materials Research Letters *3831***: 107–123. DOI: https://doi.org/10.1080/21663831.2014.912690.

[2] B.-r. Ke, Y.-c. Sun, Y. Zhang, W.-r. Wang, W.-m. Wang, P.-y. Ma, W. Ji, and Z.-y. Fu, (2021) *"Powder metallurgy of high-entropy alloys and related composites : A short review"* **International Journal of Minerals , Metallurgy and Materials *28***: 931. DOI: https://doi.org/10.1007/s12613-020-2221-y.

[3] E. P. George, W. A. Curtin, and C. C. Tasan, (2020) *"High entropy alloys: A focused review of mechanical properties and deformation mechanisms"* **Acta Materialia *188***: 435–474. DOI: 10.1016/j.actamat.2019.12.015.

[4] J. Cheng, X. Gan, S. Chen, Y. Lai, H. Xiong, and K. Zhou, (2019) *"Properties and microstructure of copper/nickel-iron-coated graphite composites prepared by electroless plating and spark plasma sintering"* **Powder Technology *343***: 705–713. DOI: 10.1016/j.powtec.2018.11.057.

[5] R. K. Duchaniya, U. Pandel, and P. Rao, (2021) *"Coatings based on high entropy alloys : An overview"* **Materials Today: Proceedings *44***: 4467–4473. DOI: 10.1016/j.matpr.2020.10.720.

[6] C. Ni, Y. Shi, J. Liu, and G. Huang, (2018) *"Characterization of Al0.5FeCu0.7NiCoCr high entropy alloy coating on aluminum alloy by laser cladding"* **Optics and Laser Technology *105***: 257–263. DOI: 10.1016/j.optlastec.2018.01.058.

[7] A. Kumar, A. Singh, and A. Suhane, (2022) *"Mechanically alloyed high entropy alloys: existing challenges and opportunities"* **Journal of Materials Research and Technology *17***: 2431–2456. DOI: https://doi.org/10.1016/j.jmrt.2022.01.141.

[8] M. Naghiyan, R. Shoja-razavi, H. Allah, and H. Jamali, (2018) *"Microstructure investigation of Inconel 625 coating obtained by laser cladding and TIG cladding methods"* **Surface & Coatings Technology *353***: 25–31. DOI: 10.1016/j.surfcoat.2018.08.061.

[9] L. Zhou, G. Ma, H. Zhao, H. Mou, J. Xu, W. Wang, Z. Xing, Y. Li, W. Guo, and H. Wang, (2024) *"Research status and prospect of extreme high-speed laser cladding technology"* **Optics and Laser Technology *168***: 109800. DOI: 10.1016/j.optlastec.2023.109800.

[10] A. A. Siddiqui and A. K. Dubey, (2021) *"Recent trends in laser cladding and surface alloying"* **Optics and Laser Technology *134***: 106619. DOI: 10.1016/j.optlastec.2020.106619.

[11] Y. He, J. Zhang, H. Zhang, and G. Song, (2017) *"Effects of Different Levels of Boron on Microstructure and Hardness of CoCrFeNiAlxCu0.7Si0.1By High Entropy Alloy Coating by Laser Cladding"* **Coatings *7***: DOI: 10.3390/coatings7010007.

[12] Y. Li, H. Liang, Q. Nie, Z. Qi, D. Deng, and H. Jiang, (2020) *"Microstructures and Wear Resistance of CoCrFeNi 2 V 0.5 Ti High Entropy Alloy Coating Prepared by Laser Cladding"* **Crystals *10***: 352. DOI: 10.3390/cryst10050352.

[13] P. Chakraborty, S. Kumar, and R. Tewari, (2022) *"Effect of Laser re-melting on the microstructure of High Entropy Alloys"* **Materials Letters *324***: 132669. DOI: 10.1016/j.matlet.2022.132669.

[14] M. Kafali, K. Mert, A. Erdogan, S. Emre, and K. Icin, (2023) *"Wear , corrosion and oxidation characteristics of consolidated and laser remelted high entropy alloys manufactured via powder metallurgy"* **Surface & Coatings Technology *467***: 129704. DOI: 10.1016/j.surfcoat.2023.129704.

[15] C. Pauzon, E. Hryha, P. Forêt, and L. Nyborg, (2019) *"Effect of argon and nitrogen atmospheres on the properties of stainless steel 316 L parts produced by laser-powder bed fusion"* **Materials and Desigh *179***: 107873. DOI: 10.1016/j.matdes.2019.107873.

[16] M. Gopinath, P. Thota, and A. K. Nath, (2019) *"Role of molten pool thermo cycle in laser surface alloying of AISI 1020 steel with in-situ synthesized TiN"* **Surface & Coatings Technology *362***: 150–166. DOI: 10.1016/j.surfcoat.2019.01.104.

[17] Q. Qiao, V. A. M. Cristino, L. M. Tam, and C. T. Kwok, (2023) **Surface & Coatings Technology *458***: 129357. DOI: 10.1016/j.surfcoat.2023.129357.

[18] P. F. Jiang, C. H. Zhang, S. Zhang, J. B. Zhang, J. Chen, and Y. Liu, (2020) *"Fabrication and wear behavior of TiC reinforced FeCoCrAlCu-based high entropy alloy coatings by laser surface alloying"* **Materials Chemistry and Physics *255***: 123571. DOI: 10.1016/j.matchemphys.2020.123571.

[19] Z. Cai, X. Cui, G. Jin, Z. Liu, Y. Li, and M. Dong, (2017) *"TEM observation on phase separation and interfaces of laser surface alloyed high-entropy alloy coating"* **Micron *103***: 84–89. DOI: 10.1016/j.micron.2017.10.001.

[20] S. Zhang, C. L. Wu, J. Z. Yi, and C. H. Zhang, (2015) *"Synthesis and characterization of FeCoCrAlCu high-entropy alloy coating by laser surface alloying"* **Surface & Coatings Technology *262***: 64–69. DOI: 10.1016/j.surfcoat.2014.12.013.

[21] F. Y. Shu, L. Wu, H. Y. Zhao, S. H. Sui, L. Zhou, J. Zhang, W. X. He, P. He, and B. S. Xu, (2018) *"Microstructure and high-temperature wear mechanism of laser cladded CoCrBFeNiSi high-entropy alloy amorphous coating"* **Materials Letters *211***: 235–238. DOI: 10.1016/j.matlet.2017.09.056.

[22] F. Shu, B. Yang, S. Dong, H. Zhao, B. Xu, F. Xu, B. Liu, P. He, and J. Feng, (2018) **Applied Surface Science *450***: 538–544. DOI: 10.1016/j.apsusc.2018.03.128.

[23] X. Li, Y. Feng, B. Liu, D. Yi, X. Yang, W. Zhang, G. Chen, Y. Liu, and P. Bai, (2019) *"In fl uence of NbC particles on microstructure and mechanical properties of AlCoCrFeNi high-entropy alloy coatings prepared by laser cladding"* **Journal of Alloys and Compounds *788***: 485–494. DOI: 10.1016/j.jallcom.2019.02.223.

[24] C. Ni, Y. Shi, J. Liu, and G. Huang, (2018) **Optics and Laser Technology *105***: 257–263. DOI: 10.1016/j.optlastec.2018.01.058.

[25] H. Zhang, Y. Pan, Y. He, and H. Jiao, (2011) *"Microstructure and properties of 6FeNiCoSiCrAlTi high-entropy alloy coating prepared by laser cladding"* **Applied Surface Science *257***: 2259–2263. DOI: 10.1016/j.apsusc.2010.09.084.

[26] S. Zhang, C. L. Wu, J. Z. Yi, and C. H. Zhang, (2015) *"Synthesis and characterization of FeCoCrAlCu high-entropy alloy coating by laser surface alloying"* **Surface & Coatings Technology *262***: 64–69. DOI: 10.1016/j.surfcoat.2014.12.013.

[27] S. Zhang, C. Wu, C. Zhang, M. Guan, and J. Tan, (2016) *"Laser surface alloying of FeCoCrAlNi high-entropy alloy on 304 stainless steel to enhance corrosion and cavitation erosion resistance"* **Optics & Laser Technology *84***: 23–31. DOI: 10.1016/j.optlastec.2016.04.011.

[28] C. L. Wu, S. Zhang, C. H. Zhang, H. Zhang, and S. Y. Dong, (2017) *"Phase evolution and properties in laser surface alloying of FeCoCrAlCuNi x high-entropy alloy on copper substrate"* **Surface & Coatings Technology *315***: 368–376. DOI: 10.1016/j.surfcoat.2017.02.068.

[29] J. Sudagar, J. Lian, and W. Sha, (2013) *"Electroless nickel , alloy , composite and nano coatings A critical review"* **Journal of Alloys and Compounds *571***: 183–204. DOI: 10.1016/j.jallcom.2013.03.107.

[30] M. A. A. Hanim. *3. 15 Electroless Plating as Surface Finishing in Electronic Packaging*. ***3***. 2017, 220–229. DOI: 10.1016/B978-0-12-803581-8.09177-3.

[31] A. E. El-nikhaily and O. A. Elkady, (2021) *"Improvement ductility and corrosion resistance of CoCrFeNi and AlCoCrFeNi HEAs by electroless copper technique"* **Journal of Materials Research and Technology *13***: 463–485. DOI: 10.1016/j.jmrt.2021.04.083.

[32] G. Dai, S. Wu, and X. Huang, (2022) *"Preparation process for high-entropy alloy coatings based on electroless plating and thermal diffusion"* **Journal of Alloys and Compounds *902***: 163736. DOI: 10.1016/j.jallcom.2022.163736.

[33] M.-D. Ger, Y. Sung, and J.-L. Ou, (2005) *"A novel process of electroless Ni P plating by nonisothermal method"* **Materials Chemistry and Physics *89***: 383–389. DOI: 10.1016/j.matchemphys.2004.09.018.

[34] H. Ding, J. Dai, T. Dai, Y. Sun, T. Lu, M. Li, X. Jia, and D. Huang, (2020) *"Effect of preheating / post-isothermal treatment temperature on microstructures and properties of cladding on U75V rail prepared by plasma cladding method"* **Surface & Coatings Technology *399***: 126122. DOI: 10.1016/j.surfcoat.2020.126122.

[35] H. Zhang, K. Mei, W. Guo, and Z. Li, (2023) *"Comparative study on microstructures and properties of air-cooled and water-cooled Fe-based plasma arc cladding layers"* **Journal of Materials Research and Technology *23***: 1599–1608. DOI: 10.1016/j.jmrt.2023.01.113.

[36] Q. Shen, J. Xue, X. Yu, Z. Zheng, and N. Ou, (2022) *"Triple-wire plasma arc cladding of Cr-Fe-Ni-Ti x high-entropy alloy coatings"* **Surface & Coatings Technology *443***: 128638. DOI: 10.1016/j.surfcoat.2022.128638.

[37] Y. Xie, X. Wen, J. Yan, B. Huang, and J. Zhuang, (2023) *"Microstructure and wear resistance of AlCoCrFeNiCuSn X high-entropy alloy coatings by plasma cladding"* **Vacuum *214***: 112176. DOI: 10.1016/j.vacuum.2023.112176.

[38] Y. Xie, X. Wen, B. Huang, and J. Zhuang, (2023) *"Microstructure , hardness and corrosion properties of AlCoCrFeNi 2 . 1 YHf high-entropy alloy coating prepared by plasma cladding"* **Materials Letters *330***: 133356. DOI: 10.1016/j.matlet.2022.133356.

[39] G. B. Darband, M. Aliofkhazraei, P. Hamghalam, and N. Valizade, (2017) *"Plasma electrolytic oxidation of magnesium and its alloys : Mechanism , properties and applications"* **Journal of Magnesium and Alloys *5***: 74–132. DOI: 10.1016/j.jma.2017.02.004.

[40] J. Li, Y. Huang, X. Meng, and Y. Xie, (2019) *"A Review on High Entropy Alloys Coatings : Fabrication Processes and Property Assessment"* **Advanced Engineering Materials *1900343***: 1–27. DOI: 10.1002/adem.201900343.

[41] Q. Fang, Y. Chen, J. Li, Y. Liu, and Y. Liu, (2018) *"Microstructure and mechanical properties of FeCoCrNiNb X high-entropy alloy coatings"* **Physica B: Physics of Condensed Matter *550***: 112–116. DOI: 10.1016/j.physb.2018.08.044.

[42] G. Mauer, R. Vaßen, and D. Stöver, (2007) *"Controlling the oxygen contents in vacuum plasma sprayed metal alloy coatings"* **Surface and Coatings Technology *201***: 4796–4799. DOI: 10.1016/j.surfcoat.2006.10.008.

[43] M. F. Morks, (2010) *"Plasma spraying of zirconia titania silica bio-ceramic composite coating for implant application"* **Materials Letters *64***: 1968–1971. DOI: 10.1016/j.matlet.2010.06.016.

[44] C. M. Hackett, G. S. Settles, and J. D. Miller, (1994) *"On the gas dynamics of HVOF thermal sprays"* **Journal of Thermal Spray Technology *3***: 299–304. DOI: 10.1007/BF02646278.

[45] S. Rech, A. Surpi, S. Vezzù, A. Patelli, A. Trentin, J. Glor, J. Frodelius, L. Hultman, and P. Eklund, (2013) *"Cold-spray deposition of Ti2AlC coatings"* **Vacuum *94***: 69–73. DOI: 10.1016/j.vacuum.2013.01.023.

[46] Y. Tao, T. Xiong, C. Sun, H. Jin, H. Du, and T. Li, (2009) *"Effect of α-Al 2 O 3 on the properties of cold sprayed Al/α-Al 2 O 3 composite coatings on AZ91D magnesium alloy"* **Applied Surface Science *256***: 261–266. DOI: 10.1016/j.apsusc.2009.08.012.

[47] A. Siao, M. Ang, C. C. Berndt, M. L. Sesso, A. Anupam, S. Praveen, R. S. Kottada, and B. S. Murty, (2015) *"Plasma-Sprayed High Entropy Alloys : Microstructure and Properties of AlCoCrFeNi and MnCoCrFeNi"* **Matellurgical and Materials Transaction A *46A***: 791–800. DOI: 10.1007/s11661-014-2644-z.

[48] L. Tian, Z. Feng, and W. Xiong, (2018) *"Microstructure, Microhardness, and Wear Resistance of AlCoCrFeNiTi/Ni60 Coating by Plasma Spraying"* **Coatings *8***: 112. DOI: 10.3390/coatings8030112.

[49] W.-l. Hsu, H. Murakami, J.-w. Yeh, A.-c. Yeh, and K. Shimoda, (2017) *"On the Study of Thermal Sprayed Ni0.2Co0.6Fe0.2CrSi0.2AlTi0.2 HEA overlay Coating"* **Surface & Coatings Technology *316***: 71–74. DOI: 10.1016/j.surfcoat.2017.02.073.

[50] M. Löbel, T. Lindner, T. Mehner, and T. Lampke, (2017) *"Microstructure and Wear Resistance of AlCoCrFeNiTi High-Entropy Alloy Coatings Produced by HVOF"* **Coatings *7***: 144. DOI: 10 . 3390 / coatings7090144.

[51] S. Yin, W. Li, B. Song, X. Yan, M. Kuang, Y. Xu, and K. Wen, (2019) *"Deposition of FeCoNiCrMn high entropy alloy (HEA) coating via cold spraying"* **Journal of Materials Science & Technology *35***: 1003–1007. DOI: 10.1016/j.jmst.2018.12.015.

[52] Y. Zou, Z. Qiu, C. Huang, D. Zeng, and R. Lupoi, (2022) *"Microstructure and tribological properties of Al 2 O 3 reinforced FeCoNiCrMn high entropy alloy composite coatings by cold spray"* **Surface & Coatings Technology *434***: 128205. DOI: 10.1016/j.surfcoat.2022.128205.

[53] M. Xue, X. Mao, Y. Lv, Y. Chi, Y. Yang, J. He, and Y. Dong, (2021) *"Comparison of Micro-nano FeCoNiCrAl and FeCoNiCrMn Coatings Prepared from Mechanical Alloyed High-entropy Alloy Powders"* **Journal of Thermal Spray Technology *30***: 1666–1678. DOI: 10.1007/s11666-021-01210-1.

[54] P. Yang, Y. Liu, X. Zhao, J. Cheng, and H. Li, (2016) *"Electromagnetic wave absorption properties of mechanically alloyed FeCoNiCrAl high entropy alloy powders"* **Advanced Powder Technology *27***: 1128–1133. DOI: 10.1016/j.apt.2016.03.023.

[55] A. Fasasi, S. Roy, A. Galerie, M. Pons, and M. Caillet, (1992) *"Laser surface alloying of Ti-6Al-4V with silicon for improved hardness and high-temperature oxidation resistance"* **Materials Letters *13***: 204–211. DOI: 10.1016/0167-577X(92)90221-5.

[56] J. Jiang, X. Feng, Y. Shen, C. Lu, and Y. Tian, (2019) *"Surface & Coatings Technology Oxidation behavior of CrAlSi12 composite coatings on Ti-6Al-4V alloy substrate fabricated via high-energy mechanical alloying method"* **Surface & Coatings Technology *367***: 212–224. DOI: 10.1016/j.surfcoat.2019.03.070.

[57] C. Shang, E. Axinte, W. Ge, Z. Zhang, and Y. Wang, (2017) *"High-entropy alloy coatings with excellent mechanical, corrosion resistance and magnetic properties prepared by mechanical alloying and hot pressing sintering"* **Surfaces and Interfaces *9***: 36–43. DOI: 10.1016/j.surfin.2017.06.012.

[58] W. Ge, B. Wu, S. Wang, S. Xu, C. Shang, Z. Zhang, and Y. Wang, (2017) *"Characterization and properties of CuZrAlTiNi high entropy alloy coating obtained by mechanical alloying and vacuum hot pressing sinterin"* **Advanced Powder Technology *28***: 2556–2563. DOI: 10.1016/j.apt.2017.07.006.

[59] A. Verma, P. Tarate, A. C. Abhyankar, M. R. Mohape, and D. S. Gowtam, (2019) *"High temperature wear in CoCrFeNiCu x high entropy alloys: The role of Cu"* **Scripta Materialia *161***: 28–31. DOI: 10.1016/j.scriptamat.2018.10.007.

[60] C.-l. Chen, (2020) *"Microstructure and mechanical properties of AlCuNiFeCr high entropy alloy coatings by mechanical alloying"* **Surface & Coatings Technology *386***: 125443. DOI: 10.1016/j.surfcoat.2020.125443.

[61] Y. Tian, C. Lu, Y. Shen, and X. Feng, (2019) *"Microstructure and corrosion property of CrMnFeCoNi high entropy alloy coating on Q235 substrate via mechanical alloying method"* **Surfaces and Interfaces *15***: 135–140. DOI: 10.1016/j.surfin.2019.02.004.

[62] E. Vmcoille, (1993) *"Dry sliding wear of TiN based ternary PVD coatings"* **Wear *165***: 41–49.

[63] A. Zhang, J. Han, B. Su, and J. Meng, (2018) *"A promising new high temperature self-lubricating material : CoCrFeNiS 0 . 5 high entropy alloy"* **Materials Science & Engineering A *731***: 36–43. DOI: 10.1016/j.msea.2018.06.030.

[64] R. Mitra and Y. R. Mahajan, (1995) *"Interfaces in discontinuously reinforced metal matrix composites: An overview"* **Bulletin of Materials Science *18***: 405–434. DOI: 10.1007/BF02749771.

[65] Z. Rahmati, H. Jamshidi Aval, S. Nourouzi, and R. Jamaati, (2022) *"Effect of copper reinforcement on the microstructure, macrotexture, and wear properties of a friction-surfaced Al-Cu-Mg coating"* **Surface and Coatings Technology *438***: 128380. DOI: 10.1016/j.surfcoat.2022.128380.

[66] H. Liu, Q. Gao, J. Dai, P. Chen, W. Gao, and J. Hao, (2022) *"Tribology International Microstructure and high-temperature wear behavior of CoCrFeNiW x high-entropy alloy coatings fabricated by laser cladding"* **Tribology International *172***: 107574. DOI: 10.1016/j.triboint.2022.107574.

[67] X. Chen, Y. Du, and Y. W. Chung, (2019) *"Commentary on using H/E and H3/E2 as proxies for fracture toughness of hard coatings"* **Thin Solid Films *688***: 137265. DOI: 10.1016/j.tsf.2019.04.040.

[68] H. T. Vo, M. Rebelo, D. Figueiredo, S. Kolozsv, P. Hosemann, and R. Franz, (2021) *"High temperature fracture toughness of single-layer CrAlN and CrAlSiN hard coatings"* **Surface & Coatings Technology *409***: 126909. DOI: 10.1016/j.surfcoat.2021.126909.

[69] C. Wang, J. Miranda, Y. Yang, and Y.-w. Chung, (2016) *"Investigation of hardness and fracture toughness properties of Fe / VC multilayer coatings with coherent interfaces"* **Surface & Coatings Technology *288***: 179–184. DOI: 10.1016/j.surfcoat.2016.01.025.

[70] S. Dal, A. Günen, N. Makuch, Y. Alt?nay, and C. Çarbo, (2022) *"Determination of fracture toughness of boride layers grown on by nanoindentation"* **Ceramics International *48***: 36410–36424. DOI: 10.1016/j.ceramint.2022.08.201.

[71] Y. Shi, B. Yang, and P. K. Liaw, (2017) *"Corrosion-resistant high-entropy alloys: A review"* **Metals *7***: 1–18. DOI: 10.3390/met7020043.

[72] M. Kafali, K. M. Doleker, A. Erdogan, S. E. Sunbul, K. Icin, A. Yildiz, and M. S. Gok, (2023) *"Wear, corrosion and oxidation characteristics of consolidated and laser remelted high entropy alloys manufactured via powder metallurgy"* **Surface and Coatings Technology *467***: 129704. DOI: 10.1016/j.surfcoat.2023.129704.

[73] W. Li, P. Liu, and P. K. Liaw, (2018) *"Microstructures and properties of high-entropy alloy films and coatings : a review"* **Materials Research Letters *3831***: 199 229. DOI: 10.1080/21663831.2018.1434248.